

Extremely metal-poor Lyman limit system at $z_{\text{abs}} = 2.917$ toward the quasar HE 0940–1050[★]

S. A. Levshakov¹, I. I. Agafonova¹, M. Centurión², and P. Molaro²

¹ Department of Theoretical Astrophysics, Ioffe Physico-Technical Institute, 194021 St. Petersburg, Russia

² Osservatorio Astronomico di Trieste, via G. B. Tiepolo 11, 34131 Trieste, Italy

Received 28 March 2002 / Accepted 25 October 2002

Abstract. We report on detailed Monte Carlo inversion analysis of the Lyman limit system observed at $z_{\text{abs}} = 2.917$ in the VLT/UVES spectrum of the quasar HE 0940–1050. Metal absorption lines of carbon and silicon in three ionization stages and numerous atomic hydrogen lines have been analyzed simultaneously. It is found that in order to match the observations, the shape of the ultraviolet background ionizing spectrum of Haardt & Madau (1996) should be modified: a spectrum with a higher intensity of the emission feature at 3 Ryd is required. It is also found that synthetic galactic spectra (or different mixtures of them with power law spectra) cannot reproduce the observations, indicating that the stellar contribution to the ionizing background is negligible at $z \sim 3$. For the first time a very low carbon abundance of $[C/H] = -2.93 \pm 0.13$ and the abundance ratio $[Si/C] = 0.35 \pm 0.15$ are directly measured in the Lyman limit system with $N(\text{H I}) = 3.2 \times 10^{17} \text{ cm}^{-2}$. If the absorber at $z_{\text{abs}} = 2.917$ provides an example of a pristine gas enriched by the nucleosynthetic products of early generations of stars, then the measured value of $[Si/C]$ seems to indicate that the initial mass functions for these stellar populations are constrained to intermediate masses, $M_{\text{up}} \lesssim 25 M_{\odot}$.

Key words. cosmology: observations – line: formation – line: profiles – galaxies: abundances – quasars: absorption lines – quasars: individual: HE 0940–1050

1. Introduction

Metal abundance measurements in quasar intervening absorbers provide insight into the chemical evolution of matter over cosmological time scales. Since heavy elements were discovered in some Ly α clouds at $z \sim 3$ by Cowie et al. (1995) and by Tytler et al. (1995), several mechanisms explaining the origin of metals in the intergalactic medium (IGM) have been proposed. Nowadays it is supposed that at $z \gtrsim 10$ the IGM was pre-enriched by the first Population III (Pop III) stars formed from gas with zero metallicity (e.g. Bromm et al. 2001; Nakamura & Umemura 2001) and enriched later due to disruption of low-mass protogalaxies (e.g. Madau et al. 2001) at $6 \lesssim z \lesssim 10$, and due to ejection of metals from massive galaxies at $z \lesssim 6$ (e.g. Aguirre et al. 2001; Scannapieco et al. 2002). It is clear that to see the signature of Pop III stars one must go to very low metallicities. The simulations of collapse and fragmentation of primordial gas clouds suggest that in the first generation the stars may have been very massive, $M_{*} \gtrsim 100 M_{\odot}$ (Abel et al. 2000; Bromm et al. 2001). However, the calculations by Nakamura & Umemura (2001) produced a bimodal

initial mass function (IMF) for Pop III stars with a second peak at $1\text{--}2 M_{\odot}$. According to these calculations the first generation supernova ($10 M_{\odot} < M_{*} < 35 M_{\odot}$) and pair-instability supernova ($140 M_{\odot} < M_{*} < 260 M_{\odot}$) can produce metallicity in the range $10^{-4}\text{--}10^{-3} Z_{\odot}$. Since the element yields and production rate differ significantly for the massive ($10\text{--}35 M_{\odot}$) and very massive ($140\text{--}260 M_{\odot}$) stars (Woosley & Weaver 1995; Umeda & Nomoto 2001; Heger & Woosley 2002), the Pop III IMF can be constrained by measuring the abundance ratios in low metallicity cosmic objects.

In the present study we report on the discovery of extremely metal-poor cloud at $z_{\text{abs}} = 2.917$ toward the quasar HE 0940–1050 which reveals the lowest metallicity of $[C/H]^1 \approx -3$ measured up to now at high redshifts. All previously reported measurements of the metal abundances in the Ly α clouds lie in the range $[C/H] > -2.4$ (Fan 1995; Songaila & Cowie 1996; Levshakov et al. 2002a, hereafter LACM; Levshakov et al. 2003, hereafter LADWD). We note that the lowest carbon abundance measured in Galactic metal poor stars is $[C/H] = -3.6$ (Norris et al. 2001).

While dealing with metallicity measurements in high redshift absorbers, one should take into account that the results are

Send offprint requests to: S. A. Levshakov,

e-mail: lev@yso.mtk.nao.ac.jp

[★] Based on observations obtained at the VLT Kueyen telescope (ESO, Paranal, Chile), the ESO programme 65.O-0474(A).

¹ Using the customary definition $[X/H] = \log(X/H) - \log(X/H)_{\odot}$. Photospheric solar abundances are taken from Holweger (2001).

strongly dependent on several assumptions on physical parameters poorly known such as geometry of the cloud, gas density distribution, shape and intensity of the background ionizing radiation, ionizing mechanisms etc. Our results are obtained with the Monte Carlo inversion (MCI) algorithms described in detail in Levshakov et al. (2000, hereafter LAK), LACM, LADWD. Since this technique is relatively new, we briefly outline here its basics.

The main assumption is that all lines observed in an absorption system arise in a *continuous* absorbing gas slab of a thickness L with a fluctuating gas density and a random velocity field. Numerous cosmological hydrodynamical calculations performed in the previous decade have shown that the QSO absorption lines arise more likely in the smoothly fluctuating intergalactic medium in a network of sheets, filaments, and halos (e.g. Cen et al. 1994; Miralda-Escudé et al. 1996; Theuns et al. 1998). This is also supported by modern high resolution spectroscopic observations: the increasing spectral resolution reveals progressively more and more complex profiles. Thus, such an approach seems to be more physically justified as compared to the model of separate homogeneous clouds which the commonly used procedure is based on. This procedure consists of the deconvolution of the complex spectra into a set of separate Voigt profiles and the subsequent estimation of ionization parameters (one for every subsystem) from the obtained ionic column densities. As shown in LAK and LACM, this simplified technique may produce incorrect metallicities exceeding in some cases 1 dex.

Further we assume that within the absorber the metal abundances are constant, the gas is in thermal and ionizing equilibrium and it is optically thin for the ionizing UV radiation. The intensity and the shape of the background ionizing radiation is considered as an external parameter. Within the absorbing region the radial velocity $v(x)$ and the total volumetric gas density $n_{\text{H}}(x)$ along the line of sight are considered as two continuous random functions which are represented by their sampled values at equally spaced intervals Δx . The computational procedure is based on the adaptive simulated annealing (see LAK, LACM), the fractional ionizations of different elements are computed at every space coordinate x with the photoionization code CLOUDY (Ferland 1997).

The MCI allows us to recover self-consistently the physical parameters of the intervening gas cloud; namely, the mean ionization parameter U_0 , the total hydrogen column density N_{H} , the line-of-sight velocity and density dispersions (σ_v and σ_y , respectively) of the absorbing gas, and the chemical abundances Z_{a} of all elements involved in the analysis. With these parameters we can further calculate the mean gas number density n_0 , the column densities for different species N_{a} , the mean kinetic temperature T_{kin} , and the linear size L . Having these comprehensive information we are able to classify the absorber more reliably and hence to obtain important clues concerning the physical conditions in the intervening clouds.

The structure of the paper is as follows. Section 2 describes the data sets, the estimated parameters for the $z_{\text{abs}} = 2.917$ Lyman limit system are given in Sect. 3, the obtained results are discussed in Sect. 4, and our conclusions are reported in Sect. 5.

2. Observations and data reduction

Observations of the QSO HE 0940–1050 ($B = 16.6$, $z_{\text{em}} = 3.06$) from the Hamburg/ESO survey (Reimers et al. 1995; Reimers et al. 1996; Reimers & Wisotzki 1997; Wisotzki et al. 2000) have been obtained with the Ultraviolet-Visual Echelle Spectrograph (UVES) on the Nasmyth focus of the ESO 8.2 m KUEYEN telescope, second unit of the VLT at Paranal, Chile.

The spectra were recorded with two different dichroic filters which allow to use the UVES blue and red arms simultaneously as two independent spectrographs for both instrumental settings. One of the instrumental configurations covered the wavelength ranges 3300–3864 Å and 4790–6816 Å with a wavelength gap between 5763 Å and 5846 Å, while the other covered the spectral regions 3740–4983 Å and 6715–10400 Å with a wavelength gap between 8530 Å and 8677 Å.

Three exposures of 3600 s each one of 2700 s were obtained for each instrumental configuration over the nights 26–29 March and 3 April 2000, when the seeing, as given by the telescope guide probe, was between 0.5 and 0.7 arcsec *FWHM*.

The slit widths were set at 1 arcsec and the CCDs were read-out in 2×2 pixel binned mode, resulting in a spectral resolution between 6.6 and 7.1 km s⁻¹. This full width at half maximum of the instrumental profile was measured from the widths of emission lines of the thorium-argon lamp used for the wavelength calibration of the spectra.

The data reduction was performed using the ECHELLE context routines implemented in the ESO MIDAS package. Flat-fielding, cosmic ray removal, sky subtraction, and wavelength calibration were performed on each spectrum separately. Typical rms of the wavelength calibration is ≤ 1 mÅ.

The observed wavelength scale of each spectrum was then transformed into vacuum, heliocentric wavelength scale. The single extracted spectra were then added together using weights proportional to their S/N . Finally, the local continuum was determined in the average spectrum by using a spline to connect smoothly the regions free from absorption features. The continuum for the Ly α forest region was fitted by using the small regions deemed to be free of absorptions and by drawing an interpolating spline between them.

We confirm the identification of several metal absorption-line systems with $z = 2.82$, 2.32, 1.918, and 1.06 performed from the low (4 Å) resolution spectra of HE 0940–1050 by Reimers et al. (1995). These systems will be analyzed in detail in a separate paper. A new Lyman limit system (LLS) with $z_{\text{abs}} = 2.917$, found in the high resolution (≈ 0.1 Å) VLT/UVES spectra, is the subject of the present work.

3. Lyman limit system at $z_{\text{abs}} = 2.917$

The Lyman limit system at $z_{\text{abs}} = 2.9171$ toward the quasar HE 0940–1050 consists of hydrogen Lyman series lines (from Ly α up to Ly-20) and metal lines of C II $\lambda 1334$, Si II $\lambda 1260$ and $\lambda 1526$ (the Si II $\lambda 1190, 1193$ lines are blended), Al II $\lambda 1670$, C III $\lambda 977$, Si III $\lambda 1206$, N III $\lambda 989$, C IV $\lambda 1548$ and $\lambda 1550$, Si IV $\lambda 1393$ and $\lambda 1402$. The doublet O VI $\lambda 1031, 1037$ is hopelessly blended and no conclusions

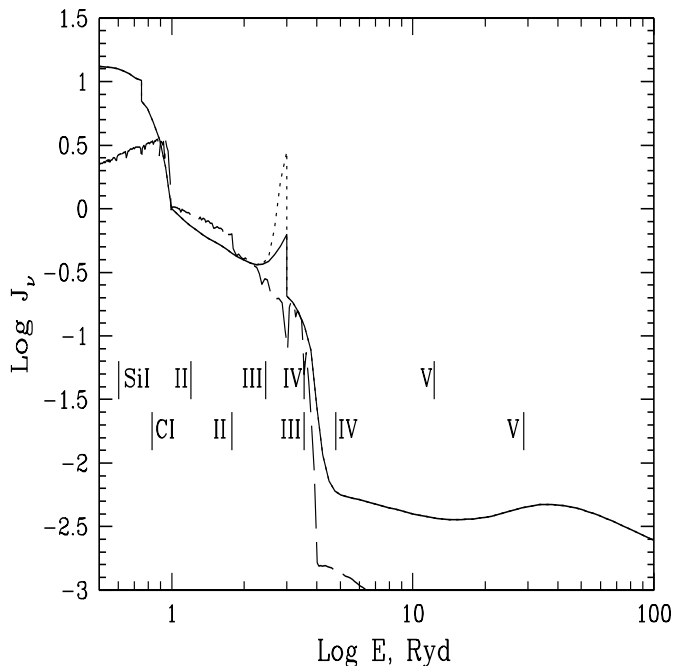


Fig. 1. UV-background ionizing continua used in the present calculations. The spectra have been normalized so that $J_\nu(h\nu = 1 \text{ Ryd}) = 1.0$. The solid curve shows the spectrum computed by Haardt & Madau (1996) at $z = 3$. The dashed curve is a galactic spectrum from Leitherer et al. (1999) shown in their Fig. 8e – spectral energy distribution at 5 Myr with $Z/Z_\odot = 0.001$. The dotted line at 3 Ryd shows the modification of the Haardt and Madau spectrum required by the present observations. The positions of tick marks of different Si and C ions are indicated by tick marks.

about this important element can be made. Additionally the quasar spectrum beyond the Lyman limit ($\lambda_{\text{obs}} < 3572.4 \text{ \AA}$) shows residual intensity $I_\lambda \approx 0.14$ giving us a model independent estimation of the total neutral hydrogen column density of about $3 \times 10^{17} \text{ cm}^{-2}$.

The first attempts to inverse the system under study were made with the HM ionizing spectrum corresponding to $z = 3$. In spite of many trials with different initial conditions it turned out to be impossible to gain a good fitting for all available lines: the Si II $\lambda 1260$ line was systematically overestimated, whereas the Si IV $\lambda 1393, 1402$ doublet – underestimated. This was the reason why we started to modify the shape of the background ionizing spectrum. After numerous experiments with different power law spectra, galactic spectra from Leitherer et al. (1999) and combinations of them it was found empirically that the self-consistent fitting of all observed lines can be achieved if we adopt the HM spectrum with about 4 times enhanced intensity between 2 and 3 Ryd (shown by the dotted line in Fig. 1). Can this emission peak be present in the real intergalactic UV background? Yes, indeed. The bump at 3 Ryd in the HM spectrum is due to He II Ly α recombination radiation produced by the photoionized Ly α forest clouds. The primary quasar UV continuum spectra were adopted by HM in the form of power law $\nu^{-1.5}$ (for $\lambda < 1216 \text{ \AA}$). But it is known that the far UV region of quasar radiation sometimes contains rather strong emission lines. For instance, quasar He II Ly α emission at 3 Ryd was

Table 1. Physical parameters of the $z_{\text{abs}} = 2.917$ Lyman limit system toward HE 0940–1050 derived by the MCI procedure.

Parameter	$z_{\text{abs}} = 2.9171$
Mean ionization parameter, U_0	$7.6\text{E-}2^c$
Total H column density, N_{H} , cm^{-2}	$3.5\text{E}20^c$
Velocity dispersion, σ_v , km s^{-1}	50.0^c
Density dispersion, σ_y	1.5^c
Chemical abundances ^d :	
Z_{C}	$4.6\text{E-}7^c$
Z_{N}	$<5.3\text{E-}8$
Z_{Al}	$5.1\text{E-}9$
Z_{Si}	$9.0\text{E-}8^c$
$[Z_{\text{C}}]$	-2.93 ± 0.13
$[Z_{\text{N}}]$	<-3.3
$[Z_{\text{Al}}]^b$	-2.76 ± 0.10
$[Z_{\text{Si}}]$	-2.58 ± 0.08
Column densities, cm^{-2} :	
$N(\text{H I})$	$(3.2 \pm 0.1)\text{E}17$
$N(\text{C II})$	$(4.8 \pm 0.3)\text{E}12$
$N(\text{Al II})$	$2.2\text{E}11$
$N(\text{Si II})$	$(1.07 \pm 0.02)\text{E}12$
$N(\text{C III})$	$(1.20 \pm 0.06)\text{E}14$
$N(\text{N III})$	$<1.4\text{E}13$
$N(\text{Si III})$	$(1.35 \pm 0.02)\text{E}13$
$N(\text{C IV})$	$(2.9 \pm 0.2)\text{E}13$
$N(\text{Si IV})$	$(6.8 \pm 0.2)\text{E}12$
Hydrogen number density, n_0 , cm^{-3}	$8.3\text{E-}4$
Mean kinetic temperature, K	$3.5\text{E}4$
Linear size, L , kpc	140^d

^a $Z_{\text{X}} = \text{X}/\text{H}$, $[Z_{\text{X}}] = \log(Z_{\text{X}}) - \log(Z_{\text{X}})_\odot$.

^b Al solar abundance from Grevesse & Sauval (1998).

^c Internal error is 15%.

^d Internal error is 20%.

observed in spectra of HS 1700+6416 (Davidsen et al. 1996; Reimers et al. 1998), Q 0302–003 (Jakobsen et al. 1994; Heap et al. 2000), and in the composite QSO spectrum (Telfer et al. 2002), the last spectrum also shows additional three wide emission features between 304 \AA and 500 \AA . Thus the strong bump at 3 Ryd can be explained qualitatively. However, to estimate its exact shape and the amplitude, calculations accounting for the presence of emission lines in far UV QSO spectra and for radiative transfer effects in an inhomogeneous universe are needed. From the analysis of the $z_{\text{abs}} = 2.917$ system we only conclude that to match all Si and C lines, about 4 times more photons with energies between 2 and 3 Ryd are required (the dotted line shown in Fig. 1 is only one possible example, the emission bump at 3 Ryd may be broader and lower as well).

Due to the large number of ionic transitions in the $z_{\text{abs}} = 2.917$ LLS and due to the very high S/N ratio this system is a sensitive probe of the shape of the background photoionizing radiation. For instance, it was impossible to describe self-consistently all observed profiles of hydrogen and metal absorption lines using any of the composite UV spectra ($\lambda < 912 \text{ \AA}$) of young galaxies from Leitherer et al. (1999) (a typical galactic spectrum is shown in Fig. 1 by the dashed line) or any of the combined spectra calculated by mixing (with

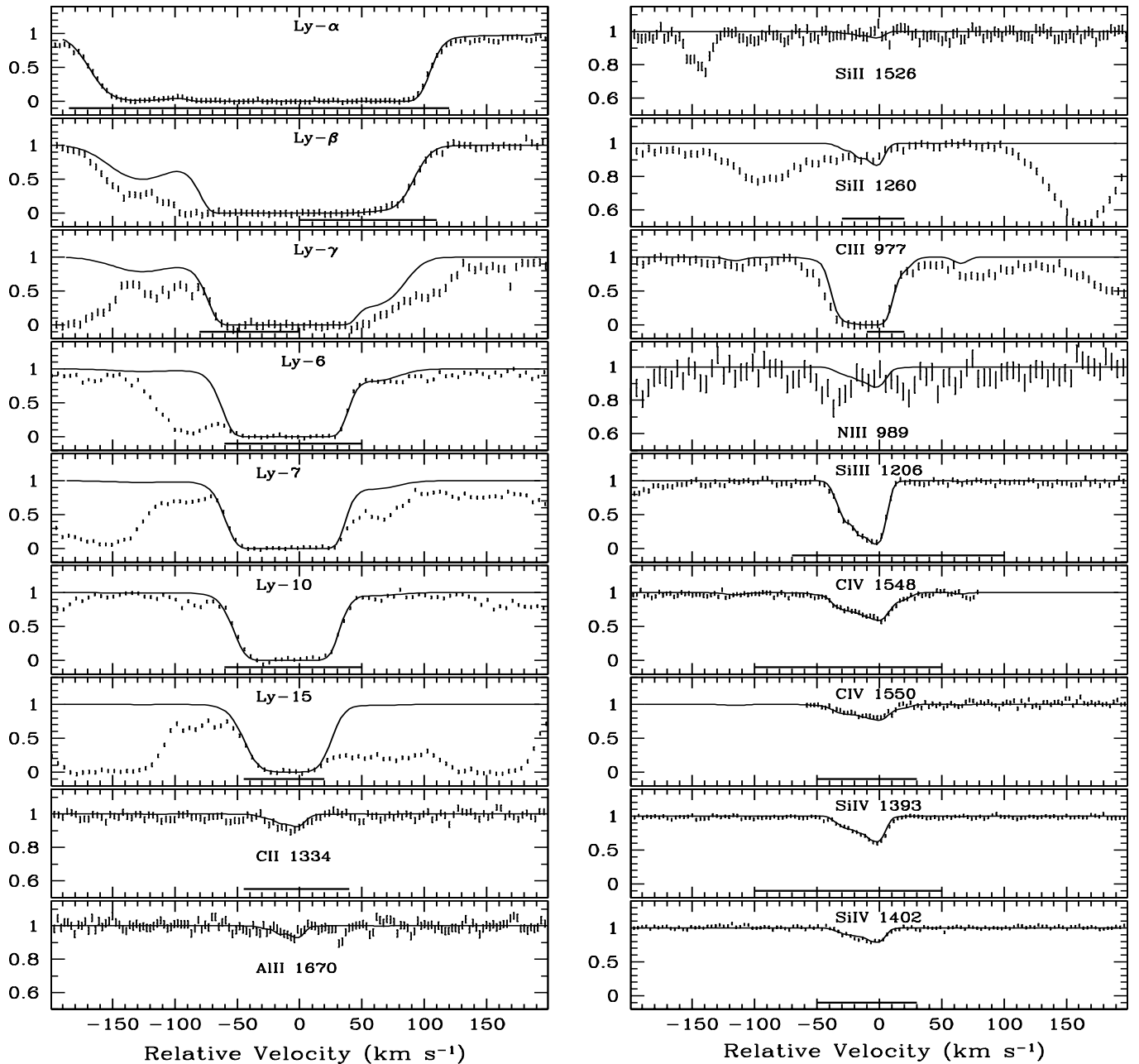


Fig. 2. Hydrogen and metal absorption lines associated with the $z_{\text{abs}} = 2.917$ LLS toward HE 0940–1050 (normalized intensities are shown by dots with 1σ error bars). The zero radial velocity is fixed at $z = 2.9171$. Smooth lines are the synthetic spectra convolved with the corresponding point-spread spectrograph function and computed with the physical parameters listed in Table 1. Bold horizontal lines mark pixels included in the optimization procedure. The normalized $\chi^2_{\text{min}} = 0.97$ (the number of degrees of freedom $\nu = 553$). Profiles of Ly- β ($\Delta v \lesssim -70$ km s $^{-1}$), Ly- γ ($\Delta v \lesssim -80$ km s $^{-1}$ and $\Delta v \gtrsim 40$ km s $^{-1}$), Ly-7 ($\Delta v \gtrsim 35$ km s $^{-1}$), Ly-15 ($\Delta v \lesssim -50$ km s $^{-1}$), and C III $\lambda 977$ ($\Delta v \lesssim -35$ km s $^{-1}$) are contaminated by other absorption lines (presumably from the Ly- α forest). The blue wing of Ly-6 ($\Delta v \lesssim -60$ km s $^{-1}$) is blended by the Ly- β line from the $z_{\text{abs}} = 2.5536$ system. The red wing of Ly-15 ($\Delta v \gtrsim 20$ km s $^{-1}$) is blended by the Ly- β and Ly-5 lines from, respectively, the $z_{\text{abs}} = 2.4962$ and 2.8237 systems (the systems with $z_{\text{abs}} = 2.4962$ and 2.5536 are identified in Agafonova et al. 2003, in preparation).

different weights) a spectrum of the young galaxy with the HM UV background. From this, we do not confirm the result by Steidel et al. (2001) that the Lyman-break galaxies produce a dominated photoionizing background at $z \sim 3$.

The results obtained with the MCI and the modified HM spectrum (Fig. 1) are presented in Table 1 and illustrated in Figs. 2–4 (for details of calculations see LAK and LACM). Parts of line profiles included in the least-squares minimization

are marked by horizontal lines in each panel in Fig. 2. We also tried to probe the presence of deuterium absorption but found that the wide Ly α profile is not sensitive to any additional D absorption. The blue wing of the Ly β line is strongly blended and this line cannot be used in the D/H estimations.

Figure 2 shows that the observed profiles (portions free from blending) are well represented. A self-consistent fitting of all available lines has revealed that the blue wing of the

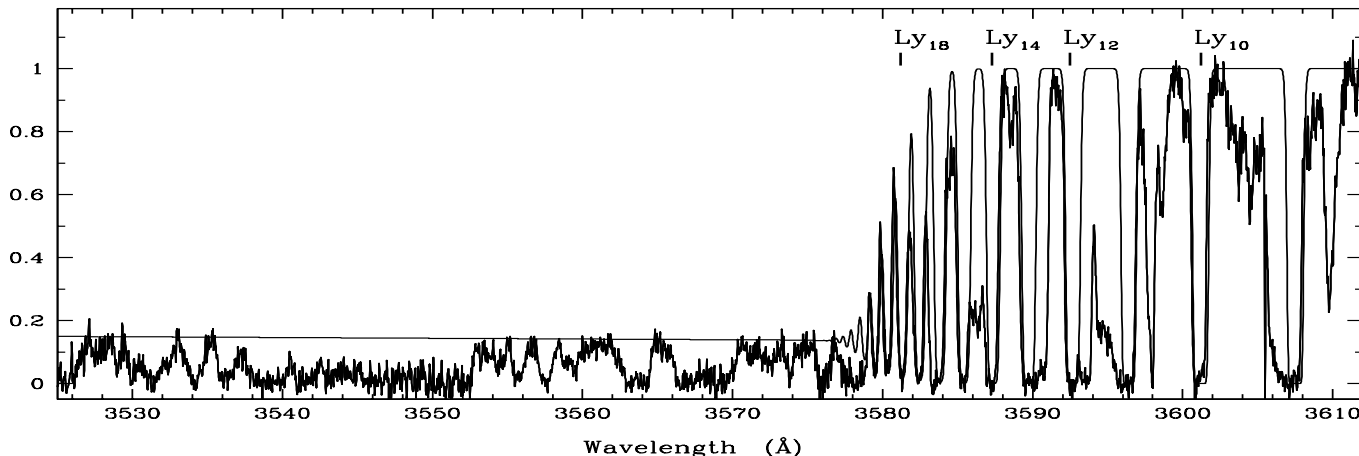


Fig. 3. Portion of the VLT/UVES spectrum of HE 0940–1050 in the region of the Lyman limit absorption at $z_{\text{abs}} = 2.917$. The panel illustrates the higher order hydrogen Lyman series lines from the $z_{\text{abs}} = 2.917$ LLS. Smooth curve represents a synthetic spectrum calculated with the physical parameters listed in Table 1. Continuum depletion between 3538 Å and 3555 Å is due to the Ly α absorption from the damped Ly α system at $z_{\text{abs}} = 1.918$.

C III $\lambda 977$ line is partly contaminated by some Ly α forest absorption.

The profiles of the Al II $\lambda 1670$ and N III $\lambda 989$ were calculated in a second round using the velocity $v(x)$ and density $n_{\text{H}}(x)$ distributions already obtained and the metallicities chosen in such a way that the synthetic spectra did not exceed 1σ deviations from the observed intensities.

The Lyman series lines higher than Ly-12 are lying on the right wing of the damped Ly α (DLA) identified at $z_{\text{abs}} = 1.918$ (Fig. 3). Using the neutral hydrogen column density in the $z_{\text{abs}} = 2.917$ LLS, we estimated the neutral hydrogen column density for the DLA system of $N(\text{H I}) \approx 1.0 \times 10^{20} \text{ cm}^{-2}$ (this DLA system is described in detail in Centurión et al. 2003).

Figure 4 illustrates the distributions of the gas density and the radial velocity inside the $z_{\text{abs}} = 2.917$ LLS. It is clearly seen that the co-existence of lowly and highly ionized species in this system is due to density fluctuations. A wide range between $x = 0.15$ and 0.37 with very low gas density is also responsible for the blue-side asymmetry seen in the metal line profiles in Fig. 2.

4. Discussion

According to the recovered parameters, the LLS at $z_{\text{abs}} = 2.917$ is a very large cloud ($L > 100 \text{ kpc}$) with very low metal content. What could it be related to?

In our code L is calculated from the ratio $L = N_{\text{H}}/n_0$, and $n_0 \propto (1 + \sigma_y^2)J_{912}/U_0$ (here J_{912} is the Lyman-limit specific intensity in $\text{erg cm}^{-2} \text{ s}^{-1} \text{ Hz}^{-1} \text{ sr}^{-1}$). Thus the intensity of the background radiation can influence the mean gas density and, hence, the absorber size. We used in our calculations $J_{912} = 0.4 \times 10^{-21} \text{ erg cm}^{-2} \text{ s}^{-1} \text{ Hz}^{-1} \text{ sr}^{-1}$ given by Haardt & Madau (1996) for the mean background intensity at $z = 3.0$. This value is poorly known and may be affected by local sources. But since we have no clues on how this value might be changed for this particular case, we will rely on the estimated linear size.

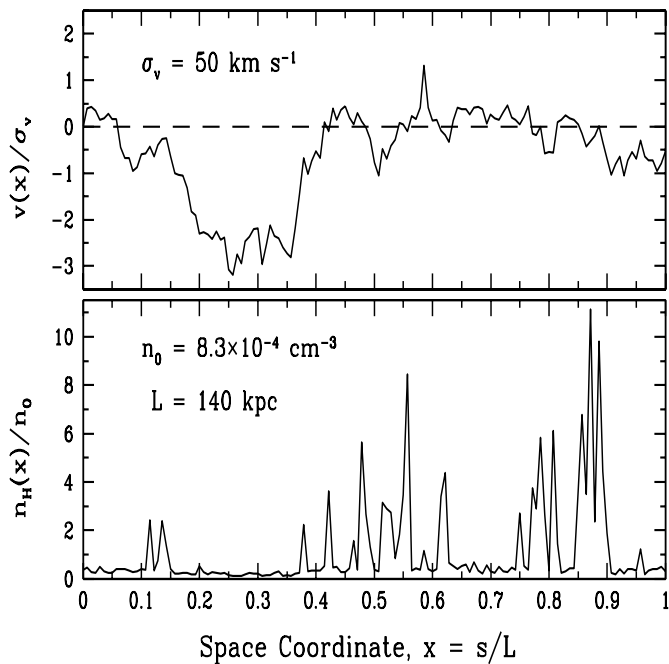


Fig. 4. Computed velocity (upper panel) and gas density (lower panel) distributions along the line of sight within the $z_{\text{abs}} = 2.917$ absorber toward HE 0940–1050. Shown are patterns rearranged according to the principle of minimum entropy production rate (see LACM).

For linear sizes as large as hundreds of kpc the velocity differences due to the Hubble expansion, Δv_{H} , become already noticeable. At $z_{\text{abs}} = 2.917$ and $L = 140 \text{ kpc}$ the velocity difference is $\Delta v_{\text{H}} = 81 \text{ km s}^{-1}$, assuming $\Omega = 1$ and the present day Hubble constant $H_0 = 75 \text{ km s}^{-1} \text{ Mpc}^{-1}$. The corresponding velocity dispersion caused by the Hubble flow is then $\sigma_{\text{H}} = \Delta v_{\text{H}} / \sqrt{12} = 23 \text{ km s}^{-1}$. The velocity dispersion of the bulk material deduced by the MCI is $\sigma_v = 50 \text{ km s}^{-1}$, implying that the line-of-sight peculiar velocity dispersion is about 44 km s^{-1} .

Large size, small peculiar velocity dispersion, and very low metallicity may indicate that the $z_{\text{abs}} = 2.917$ absorber is hosted by either an external galactic halo or by some large-scale structure object like a filament, and may consist of the gas pre-enriched by the first generations of stars. The sizes of the galactic halos or the filaments have been recently directly measured at $z < 1$. For instance, observations of C IV absorption lines by Chen et al. (2001) revealed that all these lines can be associated with galaxies seen up to 180 kpc away. Penton et al. (2002) reported on large size Ly α absorbers aligned along a possible filamentary structure of $\sim 20 h_{70}^{-1}$ Mpc long and $\sim 1 h_{70}^{-1}$ Mpc wide.

As already mentioned above, the metal content measured in this LLS may be considered as primordial, i.e. produced by the explosions of early generations of stars. Then we may use the relative metal abundances to restrict masses of these hypothetical Pop III objects. Theory predicts that the abundance ratio [Si/C] rises to highly supersolar values with increasing masses of the Pop III stars. The calculations of the nucleosynthesis patterns of metal-free stars with various masses (e.g. Umeda & Nomoto 2001) show that [Si/C] = 0.34, 0.42, 0.70 for, respectively, $M/M_{\odot} = 13, 15, 20$ (Type II SNe); [Si/C] = 0.41–0.76 for the Pop III $25 M_{\odot}$ model with explosion energies $E_{\text{exp}} = 10^{51}$ – 10^{52} erg (Fe Core Collapse Hypernovae); and [Si/C] = 1.49 and 1.70 for $M/M_{\odot} = 170$ and 200, respectively, in the Pair Instability SNe model². Similar results are reported in Heger & Woosley (2002) who also predicted a pronounced deficit of Al compared to Si ([Al/Si] $\lesssim -1.5$) in the mass range 140–260 M_{\odot} .

In our system we measured [Si/C] = 0.35 ± 0.15 and [Al/Si] = -0.18 ± 0.13 . These values certainly rule out the enrichment by very massive stars explosions and restrict the stellar masses by $\sim 25 M_{\odot}$. It should be noted that the abundance ratio [Si/C] ≈ 0.3 – 0.4 is in line with other measurements in high redshift absorbers (e.g., Songaila & Cowie 1996; Levshakov et al. 2002b, 2003). If, nevertheless, the Pop III stars were massive ($M > 140 M_{\odot}$), then the metallicity produced by their explosions should be much lower than $10^{-3} Z_{\odot}$.

We also estimated an upper limit on [N/C] < -0.4 . Nitrogen is usually assumed to be mostly produced by the intermediate mass stars ($4 \lesssim M/M_{\odot} \lesssim 8$) whereas carbon production is dominated by the massive ($M/M_{\odot} > 8$) stars (Henry et al. 2000). Unfortunately, the obtained upper limit is too high to allow us to conclude about the possible nature of nitrogen in the $z_{\text{abs}} = 2.917$ LLS: the N III $\lambda 989$ line lies in the Ly α forest where the signal-to-noise ratio is only about 25.

5. Summary

We have analyzed the VLT/UVES spectrum of the quasar HE 0940–1050 and deduced the physical properties of the

Lyman limit system at $z_{\text{abs}} = 2.917$. The main conclusions are as follows:

1. For the first time, a very low carbon abundance of [C/H] = -2.93 ± 0.13 is directly measured in the LLS providing an example of a gas cloud probably enriched by the early generations ($z > 3$) of stars.
2. The analyzed Lyman limit system has the line-of-sight size L of about 140 kpc. Its velocity dispersion is only about 50 km s^{-1} . This system may be hosted by an intergalactic filament structure or an external galactic halo.
3. The measured abundance ratios [Si/C] = 0.35 ± 0.15 and [Al/Si] = -0.18 ± 0.13 are in line with the assumption that the initial mass functions for early generations of stars are restricted to intermediate stellar masses, probably $M_{\text{up}} < 25 M_{\odot}$. The relative abundances of [Si/C] and [Al/Si] do not reveal any signature of very massive stars from the early generation.
4. The estimated shape of the photoionizing background radiation does not confirm that the Lyman-continuum radiation escaping from the young galaxies produces 5 times more H-ionizing photons per unit comoving volume than QSOs at $z \sim 3$ as suggested by Steidel et al. (2001). None of the far UV galactic spectra calculated by Leitherer et al. (1999) can produce profiles of carbon and silicon ions observed in the LLS at $z_{\text{abs}} = 2.917$.

Acknowledgements. We thank Prof. H. Habing for valuable comments and suggestions. S.A.L. gratefully acknowledges the hospitality of the National Astronomical Observatory of Japan (Mitaka) where this work was performed. The work of S.A.L. and I.I.A. is supported by the RFBR grant No. 00-02-16007.

References

- Abel, T. G., Bryan, G. L., & Norman, M. L. 2000, ApJ, 540, 39
 Aguirre, A., Hernquist, L., Schaye, J., et al. 2001, ApJ, 560, 599
 Anders, E., & Grevesse, N. 1989, Geochim. Cosmochim. Acta, 53, 197
 Bromm, V., Ferrara, A., Coppi, P. S., & Larson, R. B. 2001, MNRAS, 328, 969
 Cen, R., Miralda-Escudé, J., Ostriker, J. P., & Rauch, M. 1994, ApJ, 437, L9
 Centurión, M., Molaro, P., Vladilo, G., et al. 2003, A&A, submitted
 Chen, H.-W., Lanzetta, K. M., Webb, J. K., & Barcoux, X. 2001, ApJ, 559, 654
 Cowie, L. L., Songaila, A., Kim, T.-S., & Hu, E. 1995, AJ, 109, 1522
 Davidsen, A. F., Kriss, G. A., & Zheng, W. 1996, Nature, 380, 47
 Fan, X.-M. 1995, Ph.D. Thesis
 Ferland, G. J. 1997, A Brief Introduction to Cloudy (Internal Rep., Lexington: Univ. Kentucky)
 Grevesse, N., & Sauval, A. J. 1998, Space Sci. Rev., 85, 161
 Haardt, F., & Madau, P. 1996, ApJ, 461, 20 [HM]
 Heap, S. R., Williger, G. M., Smette, A., et al. 2000, ApJ, 534, 69
 Heger, A., & Woosley, S. E. 2002, ApJ, 567, 532
 Henry, R. B. C., Edmunds, M. G., & Köppen, J. 2000, ApJ, 541, 660
 Holweger, H. 2001, in Solar and Galactic Composition, ed. R. F. Wimmer-Schweingruber, AIP Conf. Proc., 598, 23
 Jakobsen, P., Boksenberg, A., Deharveng, J. M., et al. 1994, Nature, 370, 35

² The [Si/C] ratios from Umeda & Nomoto (2001) which are normalized to the solar abundance system given by Anders & Grevesse (1989) are adjusted to the new solar photospheric values from Holweger (2001).

- Leitherer, C., Schaerer, D., Goldader, J. D., et al. 1999, *ApJS*, 123, 3
- Levshakov, S. A., Agafonova, I. I., & Kegel, W. H. 2000, *A&A*, 360, 833 [LAK]
- Levshakov, S. A., Agafonova, I. I., Centurión, M., & Mazets, I. E. 2002a, *A&A*, 383, 813 [LACM]
- Levshakov, S. A., Dessauges-Zavadsky, M., D’Odorico, S., & Molaro, P. 2002b, *ApJ*, 565, 696
- Levshakov, S. A., Agafonova, I. I., D’Odorico, S., Wolfe, A. M., & Dessauges-Zavadsky, M. 2003, *ApJ*, 582, in press [astro-ph/0209328] [LADWD]
- Madau, P., Ferrara, A., & Rees, M. J. 2001, *ApJ*, 555, 92
- Miralda-Escudé, J., Cen, R., Ostriker, J. P., & Rauch, M. 1996, *ApJ*, 471, 582
- Nakamura, F., & Umemura, M. 2001, *ApJ*, 548, 19
- Norris, J. E., Ryan, S. G., & Beers, T. C. 2001, *ApJ*, 2001, 561, 1034
- Penton, S. V., Stocke, J. T., & Shull, J. M. 2002, *ApJ*, 565, 720
- Reimers, D., Rodríguez-Pascual, P., Hagen, H.-J., & Wisotzki, L. 1995, *A&A*, 293, L21
- Reimers, D., Köhler, T., & Wisotzki, L. 1996, *A&AS*, 115, 225
- Reimers, D., & Wisotzki, L. 1997, *Messenger*, 88, 14
- Reimers, D., Köhler, S., Hagen, H.-J., & Wisotzki, L. 1998, in Proc. of the Conf. Ultraviolet Astrophysics, Beyond the IUE Final Archive, Sevilla, Spain, 11–14 November 1997, ESA SP-413
- Savage, B. D., & Sembach, K. R. 1996, *ARA&A*, 34, 279
- Scannapieco, E., Ferrara, A., & Madau, P. 2002, *ApJ*, 574, 590
- Songaila, A., & Cowie, L. L. 1996, *AJ*, 112, 335
- Steidel, C. C., Pettini, M., & Adelberger, K. L. 2001, *ApJ*, 546, 665
- Telfer, R. C., Zheng, W., Kriss, G. A., & Davidsen, A. F. 2002, *ApJ*, 565, 773
- Theuns, T., Leonard, A., Efstathiou, G., Pearce, F. R., & Thomas, P. A. 1998, *MNRAS*, 301, 478
- Tytler, D., Fan, X.-M., Burles, S., et al. 1995, in *QSO Absorption Lines*, ed. G. Meylan (Garching: ESO), 289
- Umeda, H., & Nomoto, K. 2001, *ASP Conf. Ser.*, 222, 45
- Wisotzki, L., Christlieb, N., Bade, N., et al. 2000, *A&A*, 358, 77
- Woosley, S. E., & Weaver, T. A. 1995, *ApJS*, 101, 181